Soft Matter

Cite this: DOI: 10.1039/c2sm26523k

www.rsc.org/softmatter

COMMUNICATION

Transition from polythiophene-based one-dimensional nanofibers to spherical clusters in ultrafiltration†

Zhongcheng Pan, Jing Ge, Weihua Li, Juan Peng* and Feng Qiu*

Received 1st July 2012, Accepted 8th August 2012
DOI: 10.1039/c2sm26523k

We report the behavior of one-dimensional polythiophene-based nanofibers in solutions passing through the nanopores under a flow field. Under a strong flow field, a fiber-to-cluster transition can be observed when the nanofiber solution concentration is above a critical value. The Zimm time and the passing time of the nanofibers are compared to explain the way the nanofibers pass through the nanopores under different flow fields.

Translocation of biomacromolecules such as DNA, RNA, and proteins through nanopores is important in cell activities.[1,2] The driving forces of translocation usually involve chemical-potential difference of biomacromolecules, specific binding of proteins, and Brownian rachets with the origin from a chemical asymmetry to prevent backward diffusion.[3–6] In experiments, a voltage-driven technique is usually applied to detect such single-molecule translocations.[7,8] When the charged biomolecule in an electrolyte is translocated through the nanopores driven by the electric field, it partially blocks ion flow and is detected as a drop in the measured current. For the translocation of a synthetic polymer chain, a hydrodynamic force is used to drive the chain through the nanopores.[9,10] Due to geometric constraints, the conformation and dynamic behavior of these molecules dramatically change[11] and a first-order coil-to-stretch transition was predicted based on the blob model.[9,12] Until recently, both experimental[10] and theoretical studies[13] on translocation have mainly focused on single chains or polymer chains in solution. The translocation of the aggregated or self-assembled polymer chains with larger dimensional scale,[14] which is often involved in many industrial and laboratory processes such as mixture separation, ultrafiltration and size exclusion chromatography, is yet to be explored.

Poly(3-alkylthiophenes) (P3ATs) are one of the most promising semiconducting polymers and one-dimensional semirigid nanofibers can be formed due to strong interchain π–π stacking.[15–17] Since the optoelectronic properties of P3ATs are closely related to their structures, controlling their structures by various methods is important for further improvements in device performance.[18] The investigation on how these nanofibers of P3ATs pass through the nanopores is not only challenging in the field of ultrafiltration, but also may offer a new strategy to tailor the structure of P3ATs.

To the best of our knowledge, this is the first report of the behavior of one-dimensional P3AT-based semirigid nanofibers in solutions passing through the nanopores. A distinct structural transformation of nanofibers into spherical clusters is observed in the process of ultrafiltration under the strong flow field. In contrast, under the weak flow field or the solution concentration below a critical concentration, the nanofibers maintain a one-dimensional morphology after ultrafiltration. The remarkable effects of concentrations and flow fields on the behavior of nanofibers during ultrafiltration are then discussed using the analogy between polymer chains and nanofibers.

An all-conjugated diblock copolymer, poly(3-butylthiophene)-*b*-poly(3-dodecylthiophene) (P3BT-*b*-P3DDT) (M_n = 8200 g mol^{-1}, M_w/M_n = 1.20, f_{P3BT} = 54%), was used to form nanofibers by the whisker method.[19] Compared with P3AT homopolymers, the P3BT-*b*-P3DDT copolymer offers a better opportunity to tailor and optimize morphologies and corresponding optoelectronic properties through self-assembly.[20,21] In a typical procedure, the copolymer was dissolved in anisole (stirred at 80 °C overnight to reach sufficient dissolution and cooled to room temperature (~20 °C)) with five different concentrations (0.1, 0.2, 0.3, 0.4, and 0.5 mg mL^{-1}). Anisole is a widely used marginal solvent to prepare stably dispersed P3AT nanofibers with high aspect ratio in solvent.[19] All of them exhibit one-dimensional nanofiber morphology in solution. The ultrafiltration setup is composed of a gastight syringe and a commercial nylon membrane (~13 mm in diameter and ~110 μm in thickness) with an interpenetrating network of nanopores (~220 nm in diameter). The nanofiber solution in the syringe may pass through the membrane with either a slow macroscopic flow rate ($Q_s \approx 0.01$ mL s^{-1}) or a fast flow rate ($Q_f \approx 0.25$ mL s^{-1}), determined by the force applied on the syringe. The solution before and after ultrafiltration is analyzed by transmission electron microscopy (TEM), atomic force microscopy (AFM), dynamic laser light scattering (DLLS), and UV-vis spectroscopy.

Fig. 1(a) shows a representative TEM image of the nanofibers formed in the initial 0.2 mg mL^{-1} solution with the height, width, and length of ~3 nm, 15 nm, and 2–3 μm, respectively, measured from both TEM and AFM images (Fig. S1†). The consistent morphology measured by TEM and AFM indicated that the dry sample represented the case in the solution. These nanofibers were homogeneously distributed on the substrates, indicating their uniformly and stably

State Key Laboratory of Molecular Engineering of Polymers, Department of Macromolecular Science, Fudan University, Shanghai 200433, China. E-mail: juanpeng@fudan.edu.cn; fengqiu@fudan.edu.cn

† Electronic supplementary information (ESI) available: Experimental conditions, detailed characterization results and calculation. See DOI: 10.1039/c2sm26523k

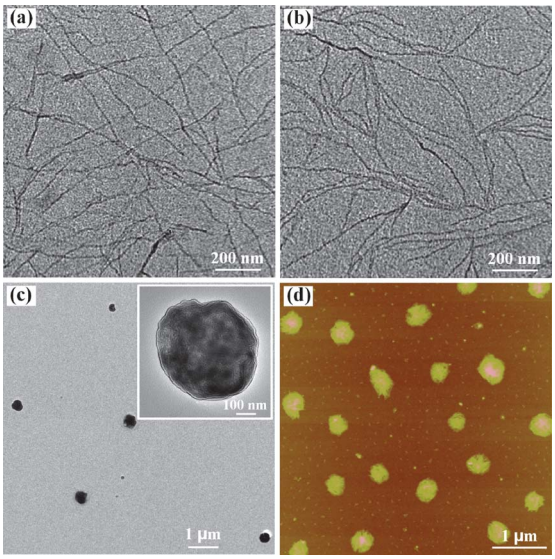

Fig. 1 (a–c) TEM and (d) AFM height images of (a) the nanofibers formed in the initial 0.2 mg mL^{-1} P3BT-*b*-P3DDT solution and after ultrafiltration at (b) $Q_s \approx 0.01$ mL s^{-1} and (c and d) $Q_f \approx 0.25$ mL s^{-1}. The inset of (c) is a magnified TEM image of a spherical cluster.

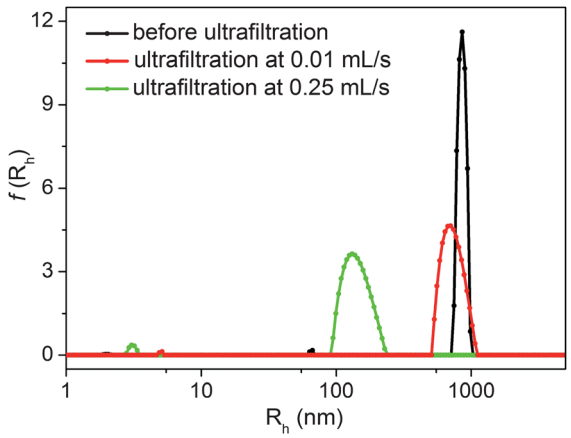

Fig. 2 Hydrodynamic radius distribution $f(R_h)$ curves obtained before and after ultrafiltration at $Q_s \approx 0.01$ mL s^{-1} and $Q_f \approx 0.25$ mL s^{-1}, respectively. The concentration of the initial P3BT-*b*-P3DDT solution is 0.2 mg mL^{-1}.

dispersed state in the solution. The cryo-TEM also shows a nanofiber morphology, further demonstrating that the nanofibers are formed in the initial solution instead of during the solvent evaporation process [Fig. S1(b)†]. When the nanofiber solution was forced to pass through the nanopores at $Q_s \approx 0.01$ mL s^{-1}, the nanofibers maintained the one-dimensional morphology [Fig. 1(b)]. However, when the flow rate was increased to ~0.25 mL s^{-1}, an obvious transformation of the nanofibers into spherical clusters was observed, with the average cluster height and diameter of 20–30 nm and 400–600 nm, respectively [Fig. 1(c) and (d)]. During the process of film preparation, the spherical cluster in solution deformed and collapsed with the evaporation of solvent. The high-magnification TEM images [Fig. 1(c), inset and Fig. S2†] show some trace of nanofibers and infer that these clusters come from the compaction of nanofibers inside the nanopores. Comparing the length of the nanofibers with the diameter of the nanopores, the semirigid nanofibers experienced confinement when passing through the nanopores.

The fiber-to-cluster transition was confirmed by DLLS, which was used to measure the average hydrodynamic radius (R_h) of nano-objects in solution (Fig. 2). The 0.2 mg mL^{-1} copolymer solution before and after ultrafiltration at the slow flow rate showed peaks of the hydrodynamic radius distribution $f(R_h)$ curves at ~850 nm and 700 nm, respectively, characteristic of the nanofibers in solutions. After ultrafiltration at the fast flow rate, the peak of the $f(R_h)$ curve shifted distinctly to ~250 nm, in agreement with the size of spherical clusters measured by TEM [Fig. 1(c)] and AFM [Fig. 1(d)]. The relative peak shift reflects the change of structures in solutions.

The TEM and AFM images show that only nanofibers existed in the original solution with a single peak of hydrodynamic radius detected by DLLS. To further prove that the spherical clusters were transformed from the nanofibers instead of existing in the original solution already, the concentrations of solutions after ultrafiltration were calibrated by UV-vis spectroscopy (Fig. S3†), which were 0.190 and 0.194 mg mL^{-1} at the slow and fast flow rates, respectively, very close to the initial value (0.2 mg mL^{-1}). It proves that there is almost no retention of the nanofibers after ultrafiltration and the spherical clusters are indeed transformed from the nanofibers.

Next we investigate the effect of the solution concentration on the process of nanofibers passing through the nanopores. In addition to 0.2 mg mL^{-1} solution, the original solutions with other concentrations (0.1, 0.3, 0.4, 0.5 mg mL^{-1}) all maintained the nanofiber morphology after ultrafiltration at $Q_s \approx 0.01$ mL s^{-1} (images not shown). At $Q_f \approx 0.25$ mL s^{-1}, however, the fiber-to-cluster transition in ultrafiltration was observed in all the investigated solutions except for the 0.1 mg mL^{-1} system (Fig. 3). By dividing the average volume of one cluster by the average volume of a single nanofiber, which is roughly estimated from the AFM measurement, there are ~3, 7, 38, and 182 nanofibers contained in one cluster in 0.2, 0.3, 0.4, and 0.5 mg mL^{-1} systems, respectively (Fig. S4†). Apparently, the size of the cluster is related to the solution concentration, however, some other factors such as the aggregation induced by flow velocity

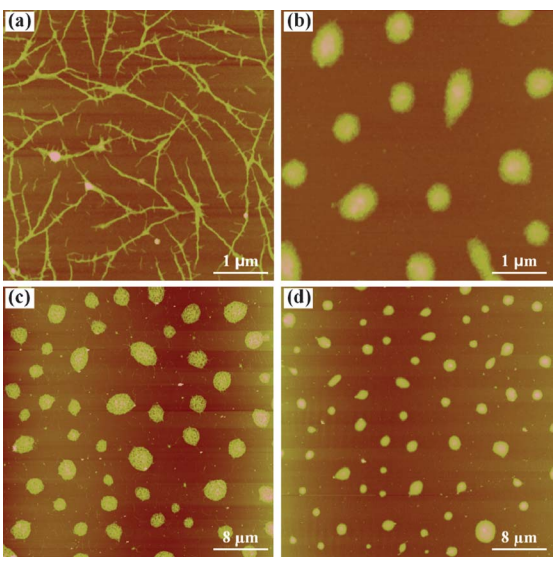

Fig. 3 AFM height images of the nanostructures formed in the P3BT-*b*-P3DDT solution with different concentrations after ultrafiltration at $Q_f \approx 0.25$ mL s^{-1}: (a) 0.1, (b) 0.3, (c) 0.4, and (d) 0.5 mg mL^{-1}.

gradient and the hydrodynamic interactions may also influence the size of the cluster.

The ultrafiltration experiments immediately raise the following interesting questions: (1) why does the 0.1 mg mL^{-1} solution always exhibit nanofiber morphology after ultrafiltration at Q_s or Q_f? (2) Why do the solutions with higher concentrations (0.2–0.5 mg mL^{-1}) exhibit a transformation of the nanofibers into spherical clusters only at Q_f? Until recently, the theory on this type of long nanofibers has not been well developed. Although the nanofiber and the polymer chain are different in the size scale, the long nanofiber can be seen as a semiflexible chain because of the similar feature of the long chain and the large aspect ratio of the nanofiber, which is comparable with that of a typical polymer chain with molecular weight around tens of thousands. In addition, the semiflexible feature can be seen from the TEM and AFM measurements. Therefore, we make a reasonable analogy between a polymer chain and a nanofiber to analyze the behavior of nanofibers during ultrafiltration.

Multiple nanofibers contained in a single cluster in 0.2–0.5 mg mL^{-1} systems indicate that the formation of spherical clusters is a typical collective behavior, during which the interpenetrating degree among the nanofibers in the initial solution plays a crucial role. The interpenetrating degree can be estimated by the average distance of nanofibers in solutions, d, relative to the size of an undisturbed single nanofiber, *i.e.*, the effective radius of gyration of a free nanofiber (R_g). When d is obviously smaller than R_g in concentrated nanofiber solutions, the nanofibers are strongly interpenetrated, and they show collective behaviors. In the opposite situation, each nanofiber behaves nearly independently. Simple estimation suggests that the nanofibers in a solution as dilute as 0.1 mg mL^{-1} are almost isolated because their average distance is comparable with R_g (refer to ESI† for calculation details) and therefore they pass through nanopores one by one during ultrafiltration under either flow rate. This explains why we did not observe the spherical clusters in the 0.1 mg mL^{-1} system at Q_s or Q_f. When increasing the concentration of the nanofiber, the increased degree of interpenetration forces multiple nanofibers to pass collectively through each nanopore. These aggregated fibers clog the nanopores easily and thus are ejected under the strong flow field, resulting in the formation of spherical clusters after ultrafiltration.

Our experimental observation reveals that the transformation of the linear fiber structure into the spherical cluster also depends on the flow rate. Under the condition of slow flow rate, no structure transition occurs. To understand the underlying mechanism, it is necessary to analyze the dynamic procedure of the nanofibers passing through nanopores. For the case of high concentrations (0.2–0.5 mg mL^{-1}), a number of nanofibers are stuck at the entrance of the nanopore at the initial stage of passing. Here we simply assume them to be a spherical region which also contains solvent molecules (Fig. 4). The spherical body mainly experiences three forces: the hydrodynamic driving force (F_h) along the flow direction, the counteracting force (F_c) from the confinement of the nanopores, and the Stokes drag force (F_s). A critical flow rate of 1.1×10^{-4} mL s^{-1}, which can be estimated from the relation of $F_h = F_c + F_s$ by using the non-draining model, is required to drive the nanofibers through the nanopores (refer to ESI† for calculation details). The estimated value is much smaller than Q_s used in our experiments. In fact, the confined nanofibers are draining, which tends to decrease the critical flow rate further. It gives a direct support to our observation that the nanofibers can pass through the nanopores under both flow rates in the experiments. By estimation, the force exerted on the nanofiber by flow is much lower than the force needed to break the nanofiber. Therefore, the fibers would not be broken during ultrafiltration (refer to ESI† for calculation details).

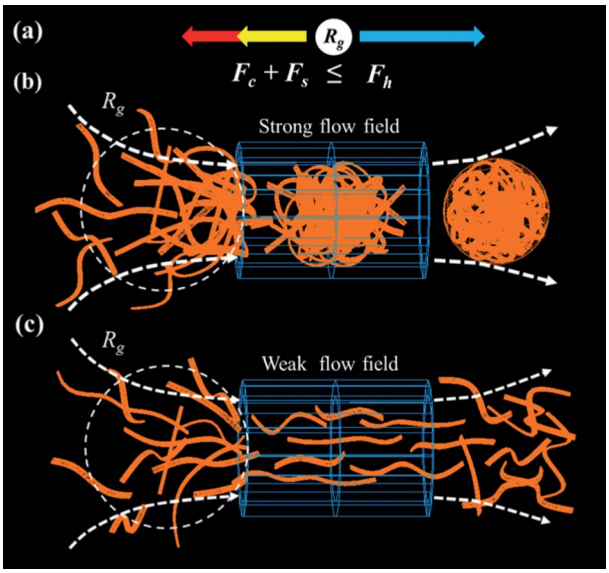

Fig. 4 Schematic representation of (a) the force balance experienced by the nanofibers in a spherical region with a radius R_g at the entrance of nanopores, and the initial nanofibers passing through a nanopore (b) under a strong flow field and (c) under a weak flow field.

To understand the structure transition further, we carry out a simple estimation to compare the passing time (τ) and the relaxation time (t_Z) of the nanofibers, which measures the time that the nanofibers take to relax themselves from an enforced configuration by the fluid flow to a favored configuration. According to the Zimm model, the t_Z can be given by the Zimm time, $t_Z \approx 0.4\eta R_g^3/K_BT$.[8,22] The passing time of the nanofibers in a spherical region of radius R_g can be estimated by $4\pi R_g^3/3q$, where q is the average microscopic flow rate inside each nanopore, *i.e.*, Q/N_{pore}. However, for a network-like membrane, it is hard to define the number of pores exactly. In an alternative way, we can estimate the effective number of pores to be $\sim 2 \times 10^8$ in the membrane according to the Hagen–Poiseuille equation (refer to ESI† for calculation details). When $t_Z \gg \tau$, the nanofibers do not have enough time to relax themselves to their favored state before they pass through the nanopore, and as a consequence, the group of nanofibers are wholly squeezed into the nanopore by the strong flow field, they further reorganize and compact themselves due to the confinement of the internal walls, and are finally thrown outside from the other side of the membrane to form spherical clusters. On the other hand, when $t_Z < \tau$, the nanofibers of enforced configuration have enough time to relax and disintegrate to an individual conformation, their original linear shape. Substituting typical values, $\eta = 0.82 \times 10^{-3}$ Pa s, $N_{pore} = 2 \times 10^8$, $T = 293$ K in our experiments, the value of t_Z/τ is about 24 at $Q_f \approx 0.25$ mL s^{-1}, and 1 at $Q_s \approx 0.01$ mL s^{-1}, respectively. It quantitatively explains our observations that the conformational transition is observed under a strong flow field [Fig. 4(b)] and on the contrary, no conformational transition occurs under a weak flow field [Fig. 4(c)].

Interestingly, these spherical clusters after ultrafiltration were stable during aging in the solution, instead of redispersing to form initial nanofiber morphology. Take the 0.2 mg mL^{-1} solution as an example, the spherical clusters seem to be amorphous without aging

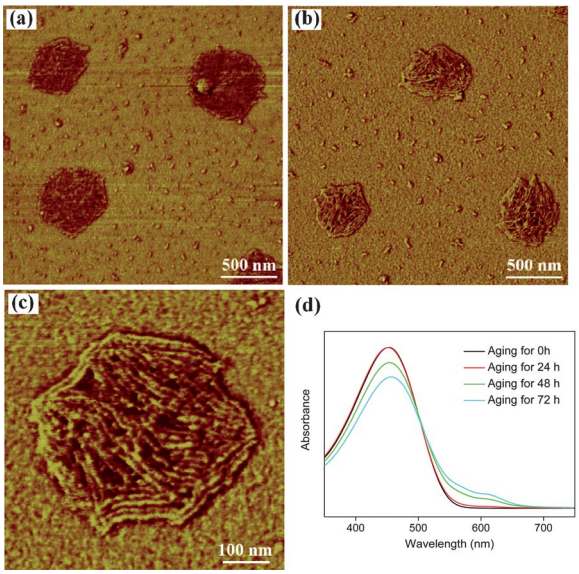

Fig. 5 AFM phase images of the spherical clusters after ultrafiltration at $Q_f \approx 0.25$ mL s^{-1} aging for (a) 0 and (b and c) 72 h. (d) UV-vis absorption spectra of the spherical cluster solution aging for different times. The concentration of the initial P3BT-*b*-P3DDT solution is 0.2 mg mL^{-1}.

[Fig. 5(a)]. With the aging time increased to 72 h, the lamellar structures completely appear on the surface of the clusters [Fig. 5(b) and (c)]. The solution of spherical clusters during aging was also investigated by UV-vis and the increased intensity of the well-resolved shoulder peak at 610 nm indicates the increased ordered structures of P3ATs in the solution [Fig. 5(d)].[15,16] After the group of nanofibers are wholly squeezed into the nanopore, entanglement between the P3AT-based nanofibers occurs.[23,24] Due to the confinement of the internal walls, the nanofibers further reorganize and compact themselves to form a whole cluster which is metastable and not disentangled after passing through the nanopore.

In summary, we have investigated the behavior of one-dimensional P3AT-based nanofibers during ultrafiltration. Both the concentration and flow field have crucial influences on the morphology after ultrafiltration. A fiber-to-cluster transition can be observed when the nanofibers in solution with the concentration above a critical value pass through the nanopores under a strong flow field, which provides a new strategy to tailor the structure of P3ATs. While under a weak flow field or the solution concentration below the critical concentration, the nanofibers maintain the one-dimensional morphology after ultrafiltration. The Zimm time and the passing time of the nanofibers are compared, which well explain the way the nanofibers pass through the nanopores under different flow fields.

Acknowledgements

This work was financially supported by the National Natural Science Foundation of China (grant no. 21074026 and 20990231). The authors are indebted to Mr Yulei Ren for TEM analysis.

Notes and references

1 G. Wang, H.-W. Chen, Y. Oktay, J. Zhang, E. L. Allen, G. M. Smith, K. C. Fan, J. S. Hong, S. W. French, J. M. McCaffery, R. N. Lightowlers, H. C. Morse III, C. M. Koehler and M. A. Teitell, *Cell*, 2010, **142**, 456.
2 D. S. Talaga and J. L. Li, *J. Am. Chem. Soc.*, 2009, **131**, 9287.
3 W. D. Richardson, A. D. Mills, S. M. Dilworth, R. A. Laskey and C. Dingwall, *Cell*, 1988, **52**, 655.
4 B. M. Simon, C. S. Peskin and G. F. Oster, *Proc. Natl. Acad. Sci. U. S. A.*, 1992, **89**, 3770.
5 W. Sung and P. J. Park, *Phys. Rev. Lett.*, 1996, **77**, 783.
6 M. Muthukumar, *J. Chem. Phys.*, 1999, **111**, 10371.
7 J. J. Kasianowicz, E. Brandin, D. Branton and D. W. Deamer, *Proc. Natl. Acad. Sci. U. S. A.*, 1996, **93**, 13770.
8 A. J. Storm, C. Storm, J. H. Chen, H. Zandbergen, J.-F. Joanny and C. Dekker, *Nano Lett.*, 2005, **5**, 1193.
9 F. Jin and C. Wu, *Phys. Rev. Lett.*, 2006, **96**, 237801.
10 H. Ge, F. Jin, J. F. Li and C. Wu, *Macromolecules*, 2009, **42**, 4400.
11 A. Milchev, *J. Phys.: Condens. Matter*, 2011, **23**, 103101.
12 P. G. De Gennes, *J. Chem. Phys.*, 1974, **60**, 5030.
13 A. K. Das and P. D. Hong, *Polymer*, 2010, **51**, 2244.
14 Q. J. Chen, H. Zhao, T. Ming, J. F. Wang and C. Wu, *J. Am. Chem. Soc.*, 2009, **131**, 16650.
15 N. Kiriy, E. Jähne, H.-J. Adler, M. Schneider, A. Kiriy, G. Gorodyska, S. Minko, D. Jehnichen, P. Simon, A. A. Fokin and M. Stamm, *Nano Lett.*, 2003, **3**, 707.
16 S. Berson, R. De Bettignies, S. Bailly and S. Guillerez, *Adv. Funct. Mater.*, 2007, **17**, 1377.
17 H. D. Tran, Y. Wang, J. M. D'Arcy and R. B. Kaner, *ACS Nano*, 2008, **2**, 1841.
18 R. Zhang, B. Li, M. C. Iovu, M. Jeffries-El, G. Sauvé, J. Cooper, S. Jia, S. Tristram-Nagle, D. M. Smilgies, D. N. Lambeth, R. D. McCullough and T. Kowalewski, *J. Am. Chem. Soc.*, 2006, **128**, 3480.
19 S. Samitsu, T. Shimomura, S. Heike, T. Hashizume and K. Ito, *Macromolecules*, 2008, **41**, 8000.
20 J. Ge, M. He, F. Qiu and Y. L. Yang, *Macromolecules*, 2010, **43**, 6422.
21 M. He, L. Zhao, J. Wang, W. Han, Y. L. Yang, F. Qiu and Z. Q. Lin, *ACS Nano*, 2010, **4**, 3241.
22 A. R. Hall, J. M. Keegstra, M. C. Duch, M. C. Hersam and C. Dekker, *Nano Lett.*, 2011, **11**, 2446.
23 W. T. Xu, H. W. Tang, H. Y. Lv, J. Li, X. L. Zhao, H. Li, N. Wang and X. N. Yang, *Soft Matter*, 2012, **8**, 726.
24 M. Koppe, C. J. Brabec, S. Heiml, A. Schausberger, W. Duffy, M. Heeney and I. McCulloch, *Macromolecules*, 2009, **42**, 4661.

